

Article

Parametric Optimization of FDM Process for Improving Mechanical Strengths Using Taguchi Method and Response Surface Method: A Comparative Investigation

Ge Gao ^{*} , Fan Xu and Jiangmin Xu

School of Mechanical Engineering, Jiangsu University of Science and Technology, Zhenjiang 212100, China

* Correspondence: gaoge@just.edu.cn

Abstract: In the present study, a comparison of two widely used optimization approaches for fused deposition modeling (FDM), that is, Taguchi method in contrast with response surface method (RSM), was investigated. Four operating parameters, namely extrusion temperature, layer thickness, raster width, print speed, and their interaction terms, were identified as control variables with three levels, while tensile strength and compressive strength were selected responses. L27 orthogonal array and face-centered central composite design (FCCCD) were used for the experimental approach for Taguchi and RSM, respectively. The signal-to-noise (S/N) ratio and analysis of variance (ANOVA) were employed to find the optimal FDM parameter combination as well as the main factor that affect the performance of the PLA samples. Based on experimental results, it was observed that conclusions about significant ranking of parameters on FDM process from these two methods were different. However, both the Taguchi method and RSM succeed in predicting better results compared with the original groups. In addition, the optimum combinations for tensile strength and compressive strength obtained from the RSM were 2.11% and 8.15% higher than Taguchi method, respectively.

Keywords: Taguchi method; response surface method; fused deposition modeling; PLA; mechanical strengths



Citation: Gao, G.; Xu, F.; Xu, J. Parametric Optimization of FDM Process for Improving Mechanical Strengths Using Taguchi Method and Response Surface Method: A Comparative Investigation. *Machines* **2022**, *10*, 750. <https://doi.org/10.3390/machines10090750>

Academic Editor: Panagiotis Kyratsis

Received: 28 July 2022

Accepted: 26 August 2022

Published: 30 August 2022

Publisher's Note: MDPI stays neutral with regard to jurisdictional claims in published maps and institutional affiliations.



Copyright: © 2022 by the authors. Licensee MDPI, Basel, Switzerland. This article is an open access article distributed under the terms and conditions of the Creative Commons Attribution (CC BY) license (<https://creativecommons.org/licenses/by/4.0/>).

1. Introduction

Additive manufacturing (AM), also known as 3D printing, can produce objects through depositing materials (e.g., powdered metal or plastic) layer by layer based on the digital model [1]. In the recent past, AM has become a rapidly emerging innovative approach in many industrial fields. Fused Deposition Modeling (FDM) is the most extensively used AM approach, which extrudes the melted filaments (e.g., plastic materials such as ABS or PLA) from the nozzle to form the component on the platform according to the prescribed manner. Due to low cost, fast fabrication, minimum energy consumption, and low material wastage, FDM technique accounts for a large proportion in the AM market. With the development of new materials and improvement of process parameters, FDM shows potential application in high-end fields such as aviation, medicine, electronics, etc. [2]. However, a well-identified limitation of the FDM products is weak mechanical properties. The input parameters play a crucial role in determining characteristics of the part quantitatively or qualitatively. Therefore, the suitable setting of parameters associated with different performances remains a challenge and must be determined.

A considerable amount of research work has been carried out to optimize and improve parameters of FDM process, and various techniques such as the Taguchi method [3,4], response surface method (RSM) [5,6], full factorial design [7–9], fractional factorial design [10,11], and other advanced techniques [12–15] have been used for analyzing and optimizing. Typically, the most widely accepted approaches are the Taguchi method and RSM, providing efficient techniques for process design and product optimization.

The Taguchi method provides an effective and reliable approach in simplification of feasibility of study and experimental plan of different process parameters. This is especially important to AM where the cost of products produced is still high. Liu et al. [16] analyzed five parameters (build orientation, layer thickness, raster width, air gap, and raster angle) on impact, flexural, and tensile strengths of ABS built parts using gray Taguchi analysis. The author observed that build orientation was the most significant parameter, followed by layer thickness and raster angle. Rinanto et al. [17] investigated the tensile strength of PLA parts for a set of extrusion temperature, raster angle, and infill density via Taguchi approach. The conclusion of their results was that 210 °C extrusion temperature, 45° raster angle, and 40% infill density maximized the performance. Deng et al. [18] designed the experiment using L9 orthogonal array for tensile properties of PEEK, and the preferable parameters were low layer thickness, high extrusion temperature, and print speed. Sood et al. [19] considered the effect of five factors namely raster width, layer thickness, air gap, raster angle, and build orientation, and their interactions on ABS dimensional accuracy via grey Taguchi method. Experimental outcomes indicated that optimal parameter settings for different mechanical characteristics were not the same. Chacón et al. [20] used a low cost printer to produce PLA samples and analyzed the important of different process parameters (layer thickness, build orientation, and print speed) and their interactions on flexural and tensile properties. The study acknowledged that the effects of build orientation and layer thickness were coupled in impacting the tensile property.

The RSM is considered another promising optimization method, which gives very low standard errors to experimental verification. The RSMs used most frequently are the central composite design (CCD) and face-centered central composite design (FCCCD). Srivastava et al. [21] determined the role of six process parameters on build time and support material via CCD. Among the analyzed parameters, raster width, contour width, layer thickness, and air gap were significant parameters, while raster angle and build orientation were deemed insignificant in comparison. Other than tensile property, Percoco et al. [22] also experimentally studied the impact of raster angle, immersion time and raster width on compressive properties of chemical dipped specimens using 3-level CCD. Their results reported that raster angle had a quite weak effect on the compressive behavior, which however increased with the increase of raster width. The functional relationships between process parameters (build orientation, layer thickness, raster angle, air gap and raster width) and strengths (tensile, flexural and impact) were determined by Sood et al. [5] and Panda et al. [23], respectively. Similar outcomes from FCCCD indicated that zero air gap and thick raster width improved the mechanical properties, while raster angle with small value was not preferable.

In fact, there are many other studies based on Taguchi and RSM that are not listed due to space limitations. Most conclusions about effects of process parameters in the review literature of FDM are also drawn according to the results of these two approaches [24–26]. From all the referred studies, the main concerns through different design of experiment (DOE) approaches usually to be answered are: (1) Among all parameters, which one has the maximum/minimum impact on FDM performance? (2) Which level of a parameter is the most beneficial to improve product's behavior? Statistical tools such as S/N analysis, ANOVA, interaction charts, and main effect plots are commonly used. However, an easily overlooked issue in FDM research is whether the conclusions obtained by different methods are the same or consistent, which have great effects on FDM parameters chosen for users and manufacturers. However, few studies focus on the comparison of different DOE approaches. Rashed et al. [27] compared Taguchi design and full factorial design to determine the influences of parameters on surface roughness and mechanical strength of Nylon 6/66 copolymer. Some errors were found in determining the influences of parameters on impact strength when using Taguchi DOE. Kechagias and Vidakis [28] assessed the efficiency of full factorial design in contrast with Box–Behnken design (BBD) of RSM in the tensile strength of PA 12 specimens, proving that, for the quadratic regression modeling, these two approaches have similar efficiency. Only in the research of Tontowi et al. [29]

were Taguchi method and RSM compared on dimensional accuracy and tensile strength by investigating raster angle, build orientation, and layer thickness. The authors recommended that RSM was a better prediction approach. However, for these existing limited articles, the above two concerned questions have not been all answered directly. To our knowledge, a comprehensive comparison between the Taguchi method and RSM has not been well-established in the literature, which remains an urgent and vital problem to be solved.

This study attempted to present the comparison between Taguchi method and RSM by analyzing FDM parameters for optimum performance of PLA samples in terms of tension and compression. Four process parameters varied on three levels, that is, extrusion temperature, layer thickness, print speed, and raster width, along with their interaction terms, were analyzed in this research. In the following, the description of experimental design through these two approaches to investigate the FDM process parameters was given. The optimal combinations with regard to mechanical characteristics, which were performed using tension and compression tests, were considered. Results were then validated by Taguchi method to determine the predictive model when compared to RSM. Statical data were discussed, and finally the study ended with the findings of the investigation.

2. Materials and Methods

2.1. Materials and Equipment

The FDM materials range includes engineering polymers (e.g., nylon and PETG), thermoplastics (e.g., PLA and ABS) and composite materials (e.g., carbon fiber composite and glass fiber composite), among which PLA is the most commonly used filament because of its biodegradability, non-toxicity, low glass transition temperature, low price, and moderate flexibility [30,31]. In this research, the material used for sample fabrication is natural PLA filament (provided by Esun Industrial Co., Ltd., Shenzhen, China) with a diameter of 1.75 mm. The FUNMAT HT 3D printer with IntamSuite slice software (provided by Intamsys Technologies Co., Ltd., Shanghai, China) is used in the study to fabricate experimental prints. Taguchi and RSM analysis are conducted using Minitab software (Version: 21.1). MIT-20 microcomputer controlled electronic universal testing machine (provided by Sanfeng Instrument Co., Ltd., Changzhou, China) is used to measure mechanical strengths, as shown in Figure 1.

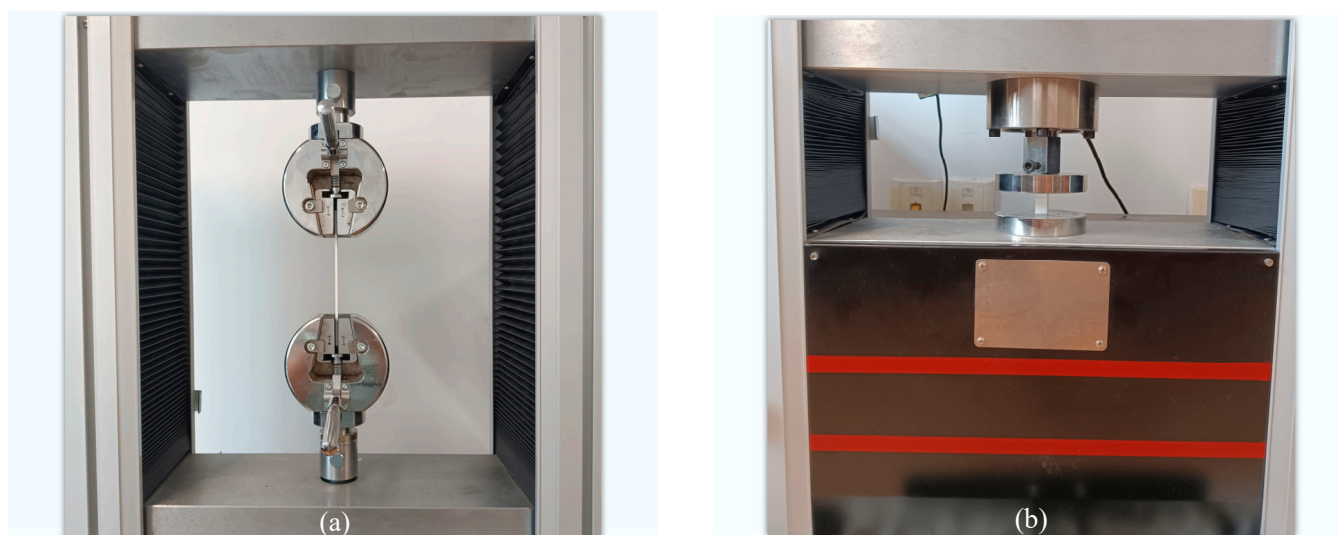


Figure 1. MIT-20 testing machine for mechanical strengths: (a) tensile; (b) compressive.

2.2. Parameters Selection

There are various parameters in FDM process found to impact mechanical characteristics of printed parts, such as infill density, air gap, number of contours, platform

temperature, etc. Meanwhile, FDM process deposits material in a criss-cross way which results in direction dependence, leading to products with anisotropy. It has been proved that the anisotropic behavior of FDM parts has close relationship with parameters such as build orientation [32], raster angle [33], and infill pattern [34]. Therefore, to exclude the interference of anisotropic property, four process parameters in Figure 2 ((A) extrusion temperature, (B) layer thickness, (C) print speed and (D) raster width) were selected as the controllable variables, which are considered to have little effect on FDM anisotropy [33]. The values for these parameters are determined based on practical experience in processing, as presented in Table 1. According to the literature, some prominent characteristics of the quality for FDM parts are mechanical strength, dimensional accuracy, surface roughness, and manufacturing time. Obviously, the mechanical strength is the most concerning and important property to the consumers, which is also selected as the response in the study.

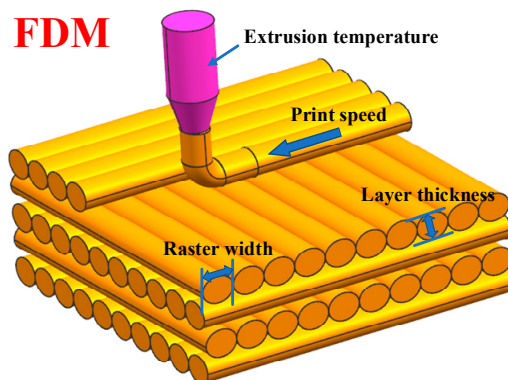


Figure 2. Graphical representation of FDM parameters.

Table 1. FDM parameters and their levels.

Symbol	FDM Parameter	Coded Levels			Unit
		−1	0	1	
A	Extrusion temperature	205	215	225	°C
B	Layer thickness	0.15	0.25	0.35	mm
C	Print speed	40	50	60	mm/s
D	Raster width	0.4	0.5	0.6	mm

2.3. Sample Preparation

Samples for strength tests were fabricated following ASTM standard, namely ASTM D638 for tensile strength and ASTM D695 for compressive strength, respectively, the dimensions of which are depicted in Figure 3. To exclude the interference of mechanical anisotropy, all samples were built at 0° raster angle with flat build orientation. A 0.6 mm nozzle diameter, 100% infill density, and 70 °C platform temperature was maintained for all prints. For a given group of parameter settings, each sample consisted of three identical specimens, which were conditioned in a laboratory environment at room temperature (24 °C) for 24 h before testing to achieve equilibrium humidity content. The mean of each experiment trial was taken as the represented value of respective strength.

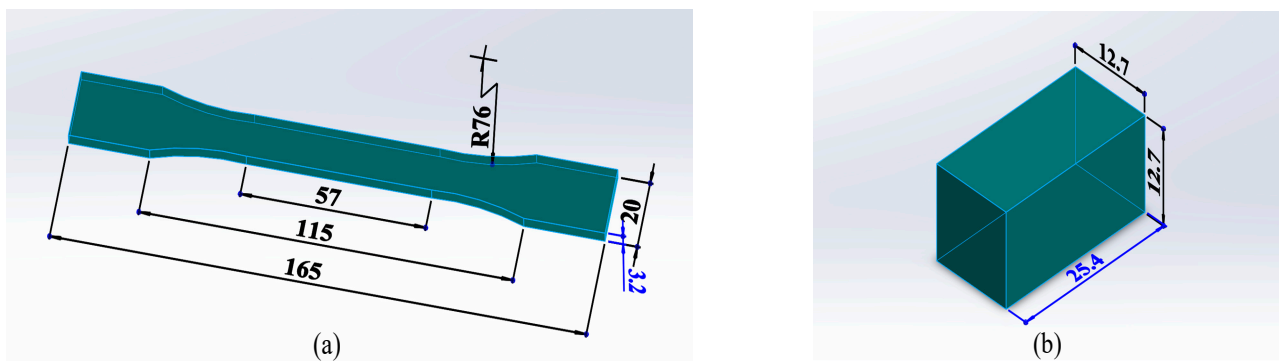


Figure 3. The dimension of the test samples: (a) tensile; (b) compressive.

3. Taguchi Method

The Taguchi method uses a fractional factorial design called orthogonal array (OA) to determine the influence of parameters and optimum combinations with fewer experiment runs. For the Taguchi method used in many FDM studies, interaction effects between control factors are often regarded as less important and can be ignored. However, some FDM parameters are dependent on the same factor and should be considered coupled. For example, print time and raster width are affected by layer thickness. Infill density significantly impact the print speed, which can be changed by adjusting raster width and air gap [24]. Therefore, it is necessary to analyze the role of the intersection effect of related parameters and in what amount it is. In this study, the effects of three interaction terms, that is, layer thickness and print speed ($B \times C$), layer thickness and raster width ($B \times D$), and print speed and raster width ($C \times D$) are taken into consideration. To select a proper orthogonal array for the experimental design, the degrees of freedom should be calculated, which can be determined as [35]:

$$DOF = (level\ number - 1) \times factor\ number + (level\ number - 1)^2 \times interaction\ number$$

For this experiment, $DOF = 2 \times 4 + 4 \times 3 = 20$. Therefore, the orthogonal array $L_{27}(3^{13})$ was used, consisting of 13 columns for assigning four single factors and three two-factor interactions. Table 2 describes the factors and levels of the Taguchi design. The experimental results of 81 specimens for mechanical strengths are tabulated in Table 3.

Table 2. Head of orthogonal array $L_{27}(3^{13})$.

Column	1	2	3	4	5	6	7	8	9	10	11	12	13
Factor	A	B	(C × D) ₂		C	(B × D) ₂		(B × C) ₁	D		(B × C) ₂	(B × D) ₁	(C × D) ₁

Table 3. Design of matrix $L_{27}(3^{13})$.

No.	A	B	C	D	Mechanical Strength (MPa)	
					Tensile	Compressive
1	−1	−1	−1	−1	34.53	21.00
2	−1	−1	0	0	35.10	19.27
3	−1	−1	1	1	36.37	21.93
4	−1	0	−1	0	35.87	20.80
5	−1	0	0	1	35.93	23.10
6	−1	0	1	−1	34.90	22.83
7	−1	1	−1	1	37.90	22.17
8	−1	1	0	−1	37.13	20.97
9	−1	1	1	0	36.80	21.67
10	0	−1	−1	0	28.83	20.10

Table 3. Cont.

No.	A	B	C	D	Mechanical Strength (MPa)	
					Tensile	Compressive
11	0	−1	0	1	33.47	20.70
12	0	−1	1	−1	31.07	21.30
13	0	0	−1	1	34.17	23.30
14	0	0	0	−1	34.70	22.73
15	0	0	1	0	33.67	21.53
16	0	1	−1	−1	35.07	22.03
17	0	1	0	0	36.17	21.67
18	0	1	1	1	34.70	22.63
19	1	−1	−1	1	35.60	22.70
20	1	−1	0	−1	25.87	19.83
21	1	−1	1	0	29.33	20.37
22	1	0	−1	−1	32.17	22.37
23	1	0	0	0	32.40	20.53
24	1	0	1	1	32.93	22.30
25	1	1	−1	0	36.50	19.07
26	1	1	0	1	36.17	18.70
27	1	1	1	−1	37.13	17.33

3.1. Results and Discussion

➤ S/N Ratio Analysis

The signal to noise ratio (S/N) is used to estimate the performance characteristics deviating from the desired values. The output of the orthogonal arrays is optimized with respect to the S/N ratio of the response. For response of mechanical strength, mean square deviation (MSD) for ‘the-larger-the-better’ quality characteristic is applied.

$$MSD = \frac{1}{n} \sum_{i=1}^n \frac{1}{y_i^2} \quad (1)$$

$$S/N = -10 \log_{10}(MSD) \quad (2)$$

where y_i is the mean mechanical strength for i_{th} set experimental sample, n is the number of experiments in the orthogonal array.

The main effect plots for mechanical strengths are shown in Figure 4. On the one hand, the S/N ratio for tensile strength (Figure 4a) decreases with increasing extrusion temperature, while it increases with increasing layer thickness and raster width. It can also be noted that, with an increase in print speed, the S/N ratio response first decreases and then increases slightly. In addition, the significances of parameters without considering interaction effects are $B > A > D > C$. The optimum combination is $A_{-1}B_1C_{-1}D_1$. When interaction terms are not ignored, the important orders are $B > A > D > (B \times D) > (C \times D) > (B \times C) > C$. The best level of partial parameters for optimum performance is $A_{-1}B_1D_1$. However, considering the interaction term $(C \times D)$ has a higher priority than C , the level of C should be given by comparing different combinations of C and D . According to the interaction plots in Figure 5, when D is set at a high level of 1, tensile strength decreases as C is changed from -1 to 1, meaning $C_{-1}D_1$ is the best combination to maximize the tensile property. That is, the optimum levels considering the interaction effect remain $A_{-1}B_1C_{-1}D_1$ (i.e., extrusion temperature 205 °C, layer thickness 0.35 mm, print speed 40 mm/s and raster width 0.6 mm).

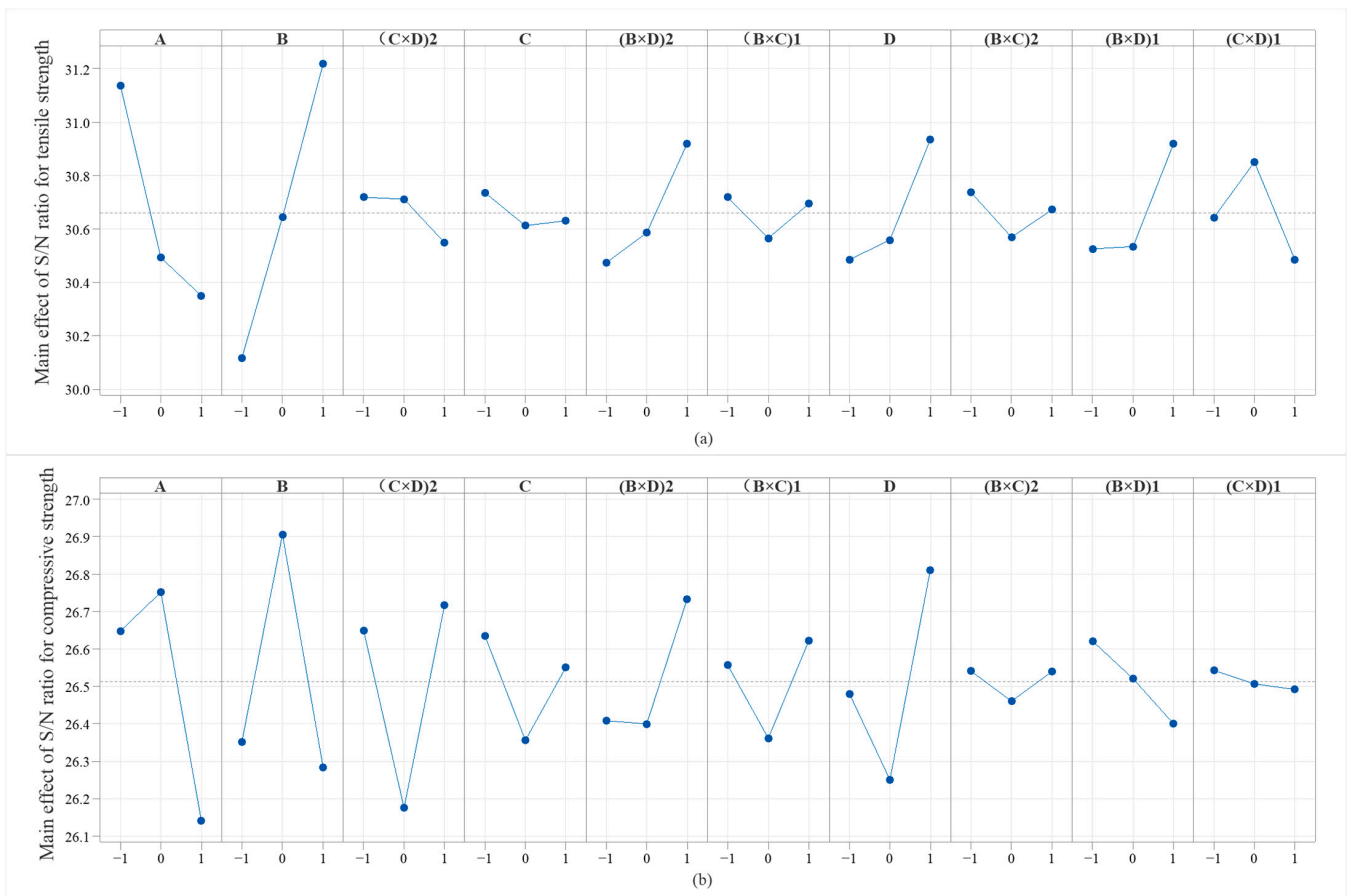


Figure 4. Main effect graph by Taguchi method: (a) tensile; (b) compressive.

On the other hand, for compressive strength (Figure 4b), the S/N ratio first increases and then decreases with increase in extrusion temperature and layer thickness. The opposite behavior is observed from print speed and raster width, respectively. The important factors sorted in descending order without interaction terms are: $B > A > D > C$. The optimum setting levels are $A_0B_0C_{-1}D_1$. When interaction effects are taken into consideration, the order becomes $B > A > D > (C \times D) > (B \times D) > C > (B \times C)$. In this situation, the optimum levels of partial parameters for compression are $A_0B_0D_1$. Since the interaction term $(C \times D)$ has a higher priority than C , therefore the optimum combination by considering the interaction effect from Figure 5 becomes $A_0B_0C_{-1}D_1$, which is also consistent with the previously unconsidered one (i.e., extrusion temperature 215 °C, layer thickness 0.25 mm, print speed 40 mm/s and raster width 0.6 mm).

Furthermore, the interactions plot in Figure 5 shows that no trends run parallel in a coupled group, which is a sign of strong interactions among the different experimental factors investigated. An interesting phenomenon is that optimum combinations are the same when considering and not considering interaction terms, both for tensile strength and compressive strength. One possible explanation is the importance of interaction term is less than individual process parameter, therefore the results remain. However, this phenomenon seems more likely to occur in Taguchi design. As we know, the orthogonal array of Taguchi's design matrix has a number limitation of factors [36] (e.g., there are at most three two-factor interactions can be investigated in $L_{27}(3^{13})$), thus it is impossible to account for all interaction effects. Since the chosen interaction terms are based on past experience and practical processing, it is likely to concentrate on unimportant interactions but neglects the significant ones. This phenomenon is more evident when compared with RSM, which will be discussed later.

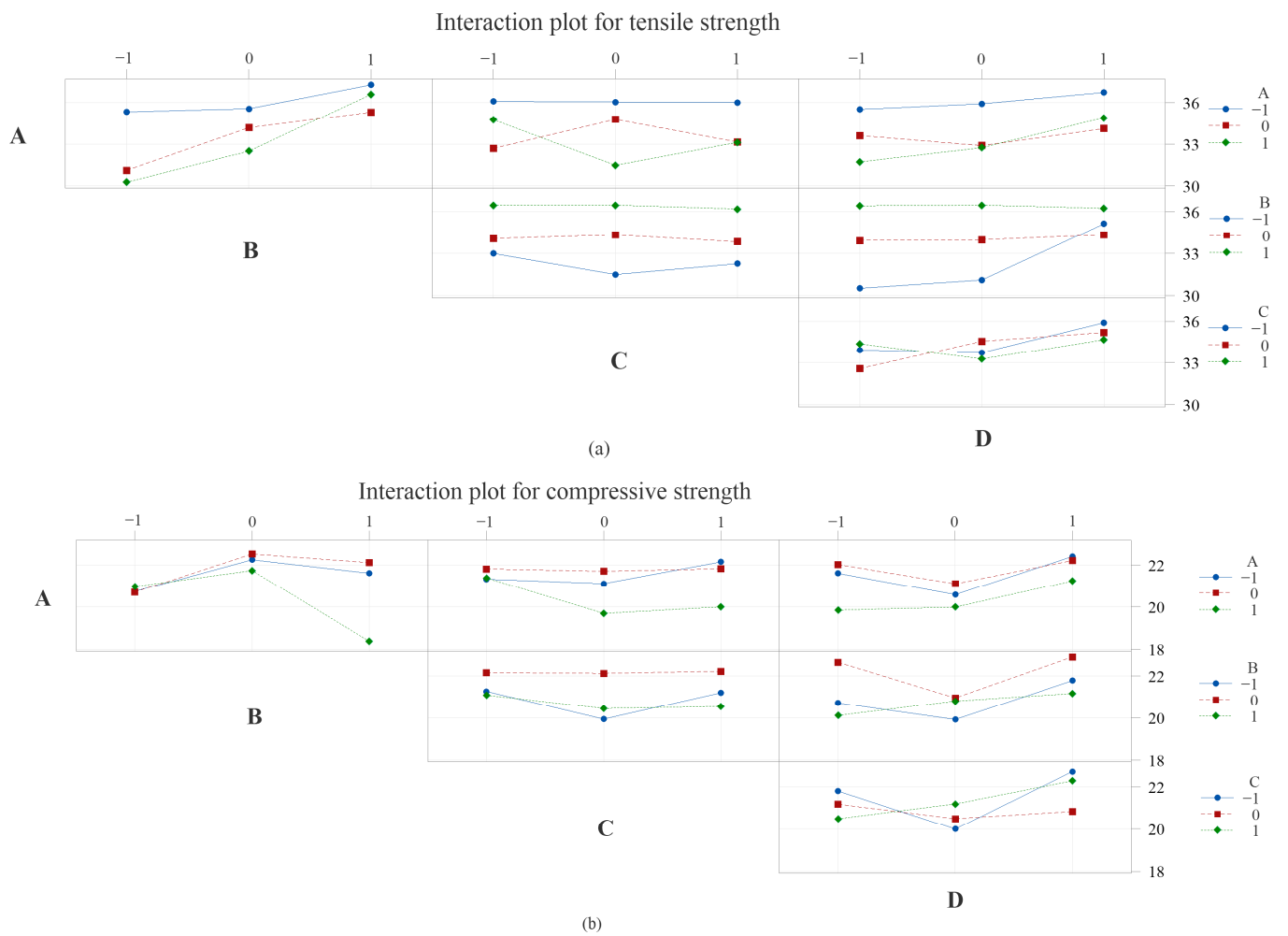


Figure 5. Interaction plot for mechanical strength by Taguchi method: (a) tensile; (b) compressive.

➤ **ANOVA Analysis**

The purpose of the analysis of variance (ANOVA) is to investigate which parameters significantly affected the quality characteristic and the relative percent influence, which has been applied at 95% confidence interval level. For importance and significance check, F value and P value given in ANOVA table are used. If P value is less than 0.05, significance of related term is established.

Observations are made from Table 4 that the significant ranking of process parameters in terms of F value by ANOVA for tension and compression is $B > A > D > (B \times D) > (C \times D) > (B \times C) > C$ and $B > A > D > (C \times D) > (B \times D) > C > (B \times C)$, respectively, which are just in agreement with results of S/N analysis before. That is, S/N analysis and ANOVA mutually verify the correctness of results of each other. In addition, for tensile strength, layer thickness (B) significantly affects the tensile strength of the specimens as P value is less than 0.05. However, for compressive strength, none of the factors are significant as their P values are all above 0.05.

Table 4. ANOVA for mechanical strengths of Taguchi method.

Factor	DOF	Tensile				Compressive				
		SS	MS	F	P	DOF	SS	MS	F	P
A	2	45.44	22.72	4.28	0.07	2	10.36	5.18	3.87	0.083
B	2	78.05	39.02	7.36	0.024	2	12.13	6.07	4.53	0.063
C	2	1.03	0.51	0.10	0.909	2	2.17	1.08	0.81	0.489
D	2	13.99	6.99	1.32	0.335	2	8.77	4.38	3.27	0.11
B × C	4	2.93	0.73	0.14	0.962	4	1.96	0.49	0.37	0.826
B × D	4	24.94	6.24	1.18	0.409	4	4.92	1.23	0.92	0.511
C × D	4	9.07	2.27	0.43	0.785	4	8.48	2.12	1.58	0.293
Errors	6	31.83	5.31			6	8.04	1.34		

DOF = degree of freedom; SS = sum of square; MS = mean sum of square.

3.2. Comparative Confirmation Test

It is found that optimum parameters and their levels just correspond to existing experiment of the orthogonal array in Table 3. That is, the optimum tension $A_{-1}B_1C_{-1}D_1$ is No.7, while the optimum compression is No.13, respectively. Furthermore, the strength values of these two settings are just the maximum of each array, proving the optimum combinations obtained from the S/N ratio analysis are correct. In terms of percentage, the difference between predicted values and actual values in Table 5 are 4.22% in tension and 1.89% in compression, respectively. Thus, these results verified the precision and efficiency of the Taguchi method.

Table 5. Confirmation experiment for Taguchi method.

	Extrusion Temperature	Layer Thickness	Print Speed	Raster Width	Predicted	Actual	Difference
Tension	205 °C	0.35 mm	40 mm/s	0.6 mm	39.50 MPa	37.9 MPa	4.22%
Compression	215 °C	0.25 mm	40 mm/s	0.6 mm	23.74 MPa	23.3 MPa	1.89%

4. Response Surface Method

4.1. Experimental Design

The empirical model for the response surface method (RSM) is usually built by central composite design (CCD), which contains five levels for each factor: zero level (center point), ± 1 level (factorial points), and $\pm \alpha$ level (axial points, or star points). Owing to machine constraints, face-centered central composite design (FCCCD) where $\alpha = 1$ is usually considered, ensuring the position of axial point on the centers of faces of the cube [23], which is also adopted in this study. In this situation, the three levels of factors for RSM are the same as the Taguchi method. These two approaches can be regarded as part of full fractional design ($3^4 = 81$ experimental runs required), which is easier for comparison on the same scale. Therefore, total 30 runs with 6 center points, 8 axial points and 16 factorial points, are used in this study, as shown in Table 6. The number of experiments required is a little more than Taguchi's.

The quadratic regression model is developed, predicting the dependent responses in terms of independent variables, along with their interactions:

$$y = \beta_0 + \sum_{i=1}^k \beta_i x_i + \sum_{i=1}^k \beta_{ii} x_i^2 + \sum_{i < j}^k \beta_{ij} x_i x_j \quad (3)$$

where y is the response; x_i is i^{th} factor with coded levels (A, B, C and D); β_0 is constant, β_i , β_{ii} and β_{ij} are the coefficient values for linear, quadratic, and interaction terms, respectively; k is the number of design factors, which is 4 in this research.

Table 6. FCCCD of RSM.

Type	No.	A	B	C	D	Mechanical Strength (MPa)	
						Tensile	Compressive
Factorial Points	1	−1	−1	−1	−1	34.53	21.00
	2	1	−1	−1	−1	30.97	24.97
	3	−1	1	−1	−1	38.07	24.92
	4	1	1	−1	−1	37.33	24.63
	5	−1	−1	1	−1	35.13	25.47
	6	1	−1	1	−1	36.73	25.20
	7	−1	1	1	−1	37.47	23.80
	8	1	1	1	−1	38.07	24.27
	9	−1	−1	−1	1	34.43	23.73
	10	1	−1	−1	1	35.60	22.70
	11	−1	1	−1	1	37.90	22.17
	12	1	1	−1	1	36.17	19.23
	13	−1	−1	1	1	36.37	21.93
	14	1	−1	1	1	33.80	24.27
	15	−1	1	1	1	35.63	21.73
	16	1	1	1	1	35.80	19.60
Axial Points	17	−1	0	0	0	33.23	21.43
	18	1	0	0	0	33.50	22.77
	19	0	−1	0	0	33.23	22.23
	20	0	1	0	0	36.73	22.87
	21	0	0	−1	0	34.03	21.70
	22	0	0	1	0	34.10	22.33
	23	0	0	0	−1	33.87	23.97
	24	0	0	0	1	33.97	23.43
Center Points	25	0	0	0	0	34.83	21.37
	26	0	0	0	0	35.10	21.87
	27	0	0	0	0	34.27	21.67
	28	0	0	0	0	33.73	21.87
	29	0	0	0	0	35.50	21.67
	30	0	0	0	0	35.40	21.73

4.2. Results and Discussion

The Anderson–Darling (AD) normality tests of the residual of the respective strength are applied. Figure 6 shows that both mechanical strengths through RSM approach fit the normality distribution, whose P values are higher than 0.05. In addition, the ANOVA from Table 7 indicates that, for tensile strength, factors with significant effects are ordered as: $B > (C \times D) > (B \times C) > B^2 > (B \times D) > (A \times C) > A > C > C^2 > D > A^2 > (A \times B) > D^2 > (A \times D)$. In the current case, P value of 0.0003 denotes extrusion temperature (A) as significant. For compressive strength, the important orders are changed as: $D > (B \times D) > (A \times B) > D^2 > B > (A \times D) > (B \times C) > (C \times D) > C > C^2 > B^2 > A > A^2 > (A \times C)$. The parameters with significant effects are D, (B × D), (A × B), and D², with P values lower than 0.05.

The conclusions about important orders of parameters are different from the Taguchi method. This can be explained as follows: On the one hand, most parameter settings of tested samples for Taguchi (27 groups) and RSM (30 groups) are different, and only four groups are the same according to the statistics, as shown in Figure 7. Therefore, the regression model for each approach, which is greatly affected by the experimental data, is different. On the other hand, the empirical model for RSM is usually full quadratic with square terms and all interaction terms, which cannot be achieved by Taguchi method. Since there are more terms to be considered in RSM, the importance of the factor is changed accordingly (For example, factor A appears in linear, square, and interaction forms in RSM). As a result, the significant rankings of parameters obtained through these two approaches are usually different, which is applicable to the optimum combination.

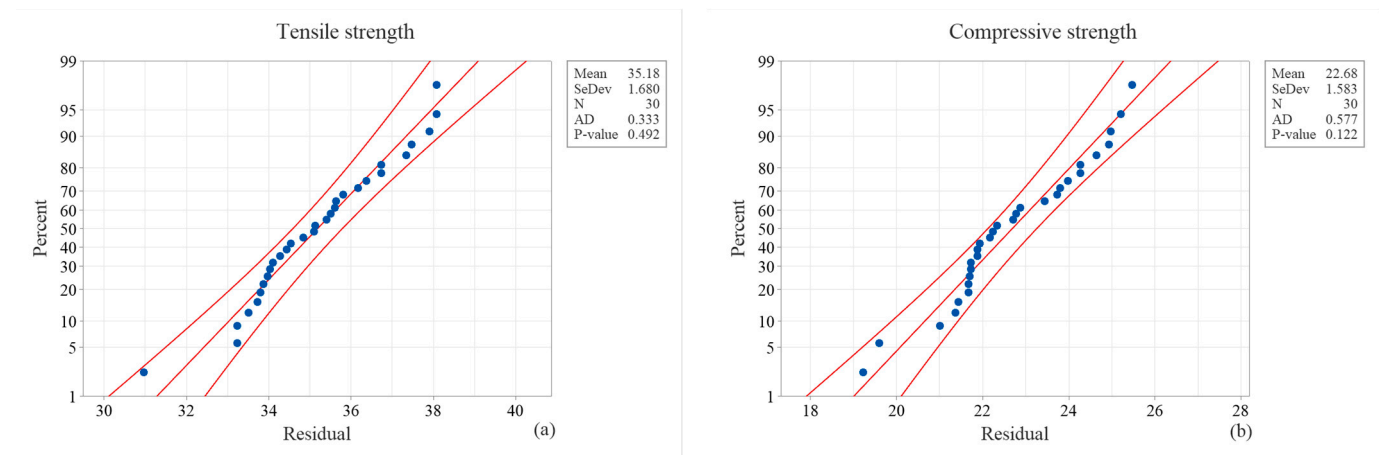


Figure 6. Normal probability plot of residual at 95% of confidence interval: (a) tensile strength, (b) compressive strength.

Table 7. ANOVA for mechanical strengths of RSM method.

Factor	Tensile					Compressive				
	DOF	SS	MS	F	P	DOF	SS	MS	F	P
A	1	1.27	1.27	1.01	0.332	1	0.12	0.12	0.11	0.742
B	1	27.83	27.83	21.96	0.0003	1	3.81	3.81	3.62	0.077
C	1	0.92	0.92	0.73	0.407	1	0.70	0.70	0.67	0.427
D	1	0.35	0.35	0.27	0.608	1	21.00	21.00	19.95	0.0005
A ²	1	0.28	0.28	0.22	0.645	1	0.11	0.11	0.11	0.75
B ²	1	4.29	4.29	3.39	0.086	1	0.15	0.15	0.15	0.708
C ²	1	0.36	0.36	0.28	0.603	1	0.22	0.22	0.21	0.654
D ²	1	0.13	0.13	0.10	0.75	1	5.03	5.03	4.78	0.045
A × B	1	0.17	0.17	0.14	0.717	1	6.13	6.13	5.82	0.029
A × C	1	1.36	1.36	1.07	0.317	1	0.03	0.03	0.03	0.867
A × D	1	0.05	0.05	0.04	0.851	1	3.65	3.65	3.47	0.082
B × C	1	5.06	5.06	4.00	0.064	1	2.27	2.27	2.15	0.163
B × D	1	4.28	4.28	3.38	0.086	1	7.40	7.40	7.03	0.018
C × D	1	5.06	5.06	4.00	0.064	1	0.77	0.77	0.74	0.405
Errors	15	19.00	1.27			15	15.79	1.05		

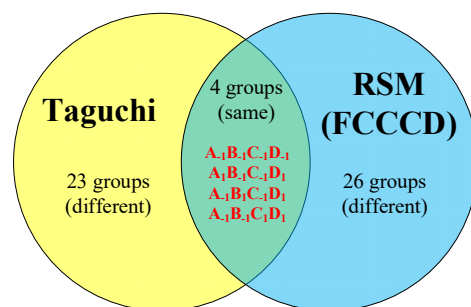


Figure 7. Relationship of experimental groups of Taguchi and RSM.

It should be pointed out that the effects of process parameters have not been discussed in this study, unlike many other studies done. This is because the conclusion of the behavior of a specific process parameter is affected by various factors, such as the DOE approach (just as this study presents), materials, environmental conditions, experimental standard, etc. Furthermore, the coupled effect of different parameter combinations will also lead to significant discrepancies. For example, Oubalouch et al. [37] investigated layer thickness, raster angle, and infill density on tensile property of PLA parts using full factorial

experiment. In the case of 10% infill density, the tensile strength was maximum at medium layer thickness. In contrast, the lower layer thickness, the higher strength was found for both 50% and 100% infill densities. Based on the same approach and material, In the study of Rajpurohit and Dave [38], the authors also determined the effect of parameters (raster width, raster angle, and layer thickness) and their interaction on tensile strength. However, experimental data showed that tensile strength and stiffness decreased with the increase of layer thickness, in spite of raster angle. Therefore, in the authors' view, discussion of the influence of parameters on FDM process without specifying the same standard/condition has minor significance for users and manufacturers, which may lead to different or even opposite conclusions.

4.3. Comparative Confirmation Test

Based on experimental data, the following regression models are developed, showing the interactions between the proposed independent variables:

$$T_S = 34.249 - 0.266A + 1.243B + 0.226C - 0.139D - 0.328A^2 + 1.287B^2 + 0.372C^2 + 0.227D^2 + 0.104(A \times B) + 0.291(A \times C) - 0.054(A \times D) - 0.563(B \times C) - 0.517(B \times D) - 0.563(C \times D) \quad (4)$$

$$C_S = 22.002 + 0.081A - 0.460B + 0.197C - 1.080D - 0.207A^2 + 0.243B^2 - 0.292C^2 + 1.393D^2 - 0.619(A \times B) + 0.044(A \times C) - 0.477(A \times D) - 0.376(B \times C) - 0.680(B \times D) - 0.220(C \times D) \quad (5)$$

The objective of the coded regression model is to properly describe the interaction of factors affecting the mechanical strength at the concentration ranges analyzed. The measured tensile strength and compressive strength vary between 30.97 MPa–38.07 Mpa and 19.23 Mpa–25.47 Mpa, respectively, which agree with the desired values as presented in Figure 8.

$$\begin{aligned} & \text{Max } T_S \text{ (or } C_S) \\ & \text{s.t. } -1 \leq A \leq 1; -1 \leq B \leq 1 \\ & \quad -1 \leq C \leq 1; -1 \leq D \leq 1 \end{aligned} \quad (6)$$

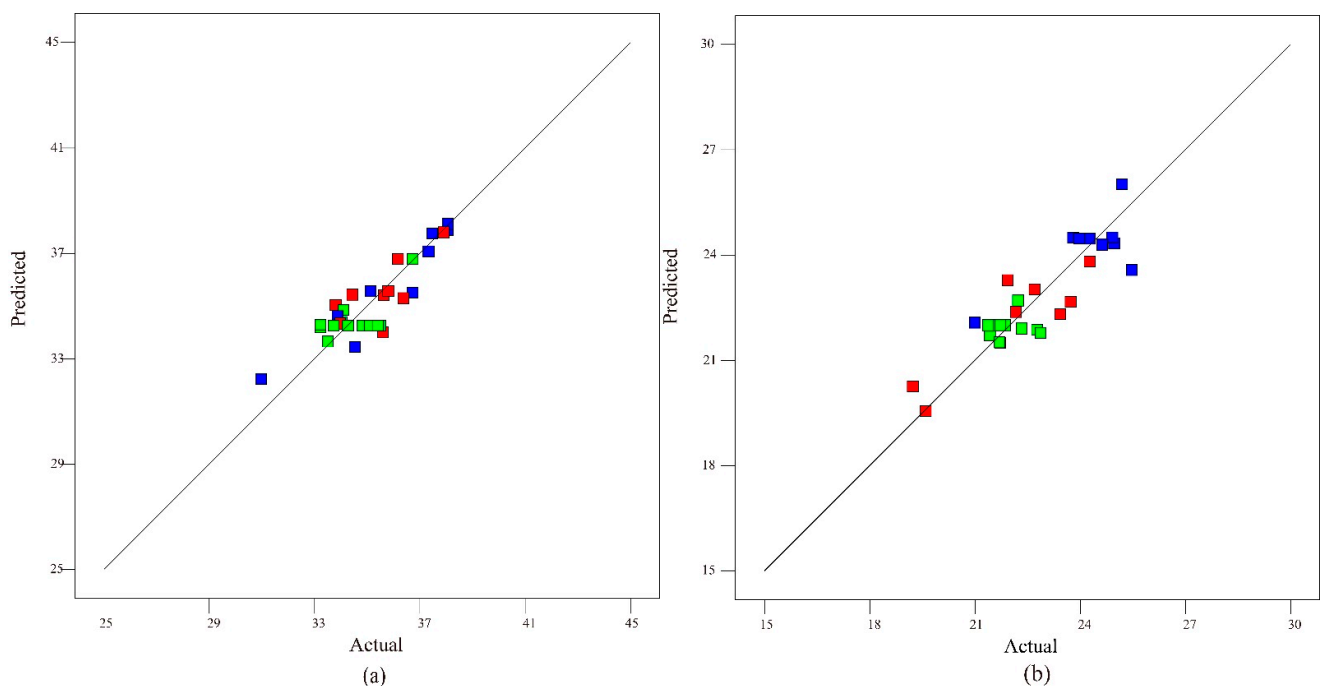


Figure 8. Predicted and actual value for mechanical strength: (a) tensile; (b) compressive.

Optimization of the experimental data is performed by making mechanical strengths be the maximum and other coded variables in range. The optimum combinations obtained from formula (6) are $A_{0.27}B_1C_1D_{-1}$ for tension and $A_1B_{-1}C_1D_{-1}$ for compression, respectively. In fact, $A_1B_{-1}C_1D_{-1}$ just corresponds to the existing experiment of No. 6 in Table 6, whose value 25.2 MPa is the second largest compressive strength, a little lower than the maximum value 25.47 MPa of No. 5. Considering experiment and measurement errors, the predicted compressive strength can be approximately deemed as the best. In comparison, for tensile strength, the optimum settings $A_{0.27}B_1C_1D_{-1}$ correspond to no existing experiment, as 0.27 is an intermediate value. Based on the optimized data presented in Table 8, the experiment was conducted to validate the prediction. Furthermore, 38.7 MPa of tensile strength is achieved, which is the maximum compared with current value in Table 6. This indicates a good agreement of the predicted and experimental values under optimum conditions.

Table 8. Confirmation experiment for RSM.

	Extrusion Temperature	Layer Thickness	Print Speed	Raster Width	Predicted	Actual	Difference
Tensile	218 °C	0.35 mm	60 mm/s	0.4 mm	38.29 MPa	38.7 MPa	1.06%
Compressive	225 °C	0.15 mm	60 mm/s	0.4 mm	26.01 MPa	25.2 MPa	3.21%

In addition, a comparison of the results with previously conducted research shows that the performance of the optimized samples is further improved by RSM than Taguchi method, in terms of both tensile strength (38.7 MPa vs. 37.9 MPa) and compressive strength (25.2 MPa vs. 23.3 MPa), indicating that RSM is a superior tool for optimizing FDM process parameters. As stated before, the regression model of RSM contains more terms than Taguchi, which facilitates fitting the characteristic curve more accurately. Moreover, unlike Taguchi method, the optimal solution of RSM can achieve any intermediate value in constraint. As a result, the optimum combination obtained by RSM is more likely to perform better, as demonstrated by the experiment.

5. Conclusions and Summary

In this work, the functional relationships between process parameters and mechanical strengths (tensile and compressive) for FDM process have been determined using the Taguchi method and RSM, respectively. The process parameters investigated are extrusion temperature, print speed, layer thickness and raster width. From this research, the following conclusions can be drawn:

(1) The Taguchi method offered 27 runs for design of experiment while RSM suggested 30 runs. Therefore, the Taguchi method can decrease the number of tests compared to RSM, even considering interaction terms. However, limited by the form of orthogonal array, Taguchi method can only consider a specific number of interaction items besides linear terms (e.g., In $L_{27}(3^{13})$, only three two-factor interactions can be investigated). In contrast, RSM can consider all interaction terms as well as quadratic terms. Therefore, the mathematical model for RSM performs better to fit the observed data.

(2) The results of significant ranking of FDM process parameters drawn by Taguchi method and RSM were different. Since most experimental data of parameter settings are different for these two approaches, the regression models are generally different, and so are the important orders of factors. Therefore, it is more meaningful to find optimum level combination by different DOE methods than to evaluate the influence of process parameter on FDM products, whose result is affected by various factors.

(3) At optimized conditions, both the Taguchi method and RSM succeed in achieving better specimen performance in terms of tension and compression, with small prediction errors. The optimum parameters from each response are as follows:

Tensile strength: Taguchi method with 37.9 MPa—205 °C extrusion temperature, 0.35 mm layer thickness, 40mm/s print speed and 0.6mm raster width; RSM with 38.7 MPa—218 °C extrusion temperature, 0.35 mm layer thickness, 60mm/s print speed and 0.4 mm raster width.

Compressive strength: Taguchi method with 23.3 MPa—215 °C extrusion temperature, 0.25 mm layer thickness, 40 mm/s print speed, and 0.6 mm raster width; RSM with 25.2 MPa—225 °C extrusion temperature, 0.15 mm layer thickness, 60 mm/s print speed, and 0.4 mm raster width.

In addition, RSM performed superiorly due to obtaining higher mechanical strengths. In fact, the optimum result of Taguchi method is essentially the permutation of existing levels for various parameters, which may lead to local optimal solution. The optimum result of RSM is more likely to achieve global optimal solution because intermediate values can be obtained (e.g., $A_{0.27}B_1C_1D_{-1}$ for tension).

Thus, it can be concluded that both the Taguchi method and RSM are robust statistical tools for FDM experimental design and process optimization. On the one hand, the Taguchi method can qualitatively show the effect of factors and determine the best level combination of parameters via S/N analysis with fewer experimental runs. However, the optimized solution obtained may miss the best result. On the other hand, RSM describes problems more quantitatively by fitting the full quadratic model via ANOVA analysis. By considering all degrees and values of factors, the global optimal condition is more likely to be achieved. However, the experiment may be time-consuming in the case of large-scale parameters.

Author Contributions: Conceptualization: G.G.; methodology: G.G.; formal analysis and investigation: F.X.; writing—original draft preparation: F.X.; writing—review and editing: G.G. and F.X.; resources: J.X.; supervision: J.X. All authors have read and agreed to the published version of the manuscript.

Funding: This research received no external funding.

Institutional Review Board Statement: Not applicable.

Informed Consent Statement: Not applicable.

Data Availability Statement: Not applicable.

Acknowledgments: This work is supported by Jiangsu Provincial Double-Innovation Doctor Program. The authors wish to express their appreciation to Yumei Wu at Jiangsu University of Science and Technology for her valuable comments.

Conflicts of Interest: The authors declare no conflict of interest.

References

1. Ngo, T.D.; Kashani, A.; Imbalzano, G.; Nguyen, K.T.; Hui, D. Additive manufacturing (3d printing): A review of materials, methods, applications and challenges. *Compos. Part. B-Eng.* **2018**, *143*, 172–196. [[CrossRef](#)]
2. Gordelier, T.J.; Thies, P.R.; Turner, L.; Johanning, L. Optimising the fdm additive manufacturing process to achieve maximum tensile strength: A state-of-the-art review. *Rapid. Prototyp. J.* **2019**, *25*, 953–971. [[CrossRef](#)]
3. Lee, B.H.; Abdullah, J.; Khan, Z.A. Optimization of rapid prototyping parameters for production of flexible ABS object. *J. Mater. Process. Tech.* **2005**, *169*, 54–61. [[CrossRef](#)]
4. Kafshgar, A.R.; Rostami, S.; Aliha, M.R.M.; Berto, F. Optimization of properties for 3d printed pla material using taguchi, anova and multi-objective methodologies. *Procedia Struct. Integr.* **2021**, *34*, 71–77. [[CrossRef](#)]
5. Sood, A.K.; Ohdar, R.K.; Mahapatra, S.S. Parametric appraisal of mechanical property of fused deposition modelling processed parts. *Mater. Design.* **2010**, *31*, 287–295. [[CrossRef](#)]
6. Equbal, A.; Sood, A.K.; Equbal, M.I.; Badruddin, I.A.; Khan, Z.A. RSM based investigation of compressive properties of fdm fabricated part. *CIRP J. Manuf. Sci. Technol.* **2021**, *35*, 701–714. [[CrossRef](#)]
7. Gurralla, P.K.; Regalla, S.P. Optimization of support material and build time in fused deposition modeling (fdm). *Appl. Mech. Mater.* **2012**, *110*, 2245–2251. [[CrossRef](#)]
8. Rayegani, F.; Onwubolu, G.C. Fused deposition modelling (fdm) process parameter prediction and optimization using group method for data handling (gmdh) and differential evolution (de). *Int. J. Adv. Manuf. Technol.* **2014**, *73*, 509–519. [[CrossRef](#)]
9. Babu, J.J.; Mehrpouya, M.; Pijper, T.C.; Willemsen, G.; Vaneker, T. An experimental study of downfacing surfaces in selective laser melting. *Adv. Eng. Mater.* **2022**, *24*, 2101562. [[CrossRef](#)]
10. Mohamed, O.A.; Masood, S.H.; Bhowmik, J.L.; Nikzad, M.; Azadmanjiri, J. Effect of process parameters on dynamic mechanical performance of fdm pc/abs printed parts through design of experiment. *J. Mater. Eng. Perform.* **2016**, *25*, 2922–2935. [[CrossRef](#)]
11. Mazen, A.; McClanahan, B.; Weaver, J.M. Factors affecting ultimate tensile strength and impact toughness of 3d printed parts using fractional factorial design. *Int. J. Adv. Manuf. Tech.* **2022**, *119*, 2639–2651. [[CrossRef](#)]

12. Giri, J.; Shahane, P.; Jachak, S.; Chadge, R.; Giri, P. Optimization of fdm process parameters for dual extruder 3d printer using artificial neural network. *Mater. Today Process.* **2021**, *43*, 3242–3249. [[CrossRef](#)]
13. Aminzadeh, A.; Aberoumand, M.; Rahmatabadi, D.; Moradi, M. Metaheuristic approaches for modeling and optimization of fdm process. In *Fused Deposition Modeling Based 3d Printing*; Dave, H.K., Davim, J.P., Eds.; Springer: Cham, Switzerland, 2021; ISBN 978-3-030-68024-4.
14. Ulu, E.; Korkmaz, E.; Yay, K.; Burak Ozdoganlar, O.; Burak Kara, L. Enhancing the structural performance of additively manufactured objects through build orientation optimization. *J. Mech. Design.* **2015**, *137*, 111410. [[CrossRef](#)]
15. Chohan, J.S.; Mittal, N.; Kumar, R.; Singh, S.; Sharma, S.; Dwivedi, S.P.; Saxena, A.; Chattopadhyaya, S.; Ilyas, R.A.; Le, C.H.; et al. Optimization of fff process parameters by naked mole-rat algorithms with enhanced exploration and exploitation capabilities. *Polymers* **2021**, *13*, 1702. [[CrossRef](#)]
16. Liu, X.; Zhang, M.; Li, S.; Si, L.; Peng, J.; Hu, Y. Mechanical property parametric appraisal of fused deposition modeling parts based on the gray taguchi method. *Int. J. Adv. Manuf. Tech.* **2017**, *89*, 2387–2397. [[CrossRef](#)]
17. Rinanto, A.; Nugroho, A.; Prasetyo, H.; Pujiyanto, E. Simultaneous optimization of tensile strength, energy consumption and processing time on fdm process using taguchi and pcr-topsis. In Proceedings of 4th International Conference on Science and Technology (ICST) IEEE, Yogyakarta, Indonesia, 7–8 August 2018; pp. 1–5. [[CrossRef](#)]
18. Deng, X.; Zeng, Z.; Peng, B.; Yan, S.; Ke, W. Mechanical properties optimization of poly-ether-ether-ketone via fused deposition modeling. *Materials* **2018**, *11*, 216. [[CrossRef](#)]
19. Sood, A.K.; Ohdar, R.K.; Mahapatra, S.S. Improving dimensional accuracy of fused deposition modelling processed part using grey taguchi method. *Mate. Design.* **2009**, *30*, 4243–4252. [[CrossRef](#)]
20. Chacón, J.M.; Caminero, M.A.; García-Plaza, E.; Núñez, P.J. Additive manufacturing of pla structures using fused deposition modelling: Effect of process parameters on mechanical properties and their optimal selection. *Mater. Design.* **2017**, *124*, 143–157. [[CrossRef](#)]
21. Srivastava, M.; Rathee, S.; Maheshwari, S.; Kundra, T.K. Multi-objective optimisation of fused deposition modelling process parameters using rsm and fuzzy logic for build time and support material. *Int. J. Rapid. Manuf.* **2018**, *7*, 25–42. [[CrossRef](#)]
22. Percoco, G.; Lavecchia, F.; Galantucci, L.M. Compressive properties of fdm rapid prototypes treated with a low cost chemical finishing. *Res. J. Appl. Sci. Eng. Technol.* **2012**, *4*, 3838–3842.
23. Panda, S.K.; Padhee, S.; Sood, A.K.; Mahapatra, S.S. Optimization of fused deposition modelling (fdm) process parameters using bacterial foraging technique. *Int. Inf. Manag.* **2009**, *1*, 89–97. [[CrossRef](#)]
24. Gao, G.; Xu, F.; Xu, J.; Tang, G.; Liu, Z. A survey of the influence of process parameters on mechanical properties of fused deposition modeling parts. *Micromachines* **2022**, *13*, 553. [[CrossRef](#)] [[PubMed](#)]
25. Bakır, A.A.; Atik, R.; Özerinç, S. Mechanical properties of thermoplastic parts produced by fused deposition modeling: A review. *Rapid. Prototyp. J.* **2021**, *27*, 537–561. [[CrossRef](#)]
26. Syrlybayev, D.; Zharylkassyn, B.; Seisekulova, A.; Akhmetov, M.; Perveen, A.; Talamona, D. Optimisation of strength properties of fdm printed parts—a critical review. *Polymers* **2021**, *13*, 1587. [[CrossRef](#)] [[PubMed](#)]
27. Rashed, K.; Kafi, A.; Simons, R.; Bateman, S. Fused filament fabrication of nylon 6/66 copolymer: Parametric study comparing full factorial and taguchi design of experiments. *Rapid. Prototyp. J.* **2022**, *28*, 1111–1128. [[CrossRef](#)]
28. Kechagias, J.D.; Vidakis, N. Parametric optimization of material extrusion 3d printing process: An assessment of box-behnken vs. full-factorial experimental approach. *Int. J. Adv. Manuf. Tech.* **2022**, *121*, 3163–3172. [[CrossRef](#)]
29. Tontowi, A.E.; Ramdani, L.; Erdizon, R.V.; Baroroh, D.K. Optimization of 3d-printer process parameters for improving quality of polylactic acid printed part. *Int. J. Eng. Technol.* **2017**, *9*, 589–600. [[CrossRef](#)]
30. Barletta, M.; Gisario, A.; Mehrpouya, M. 4D printing of shape memory polylactic acid (pla) components: Investigating the role of the operational parameters in fused deposition modelling (fdm). *J. Manuf. Process.* **2021**, *61*, 473–480. [[CrossRef](#)]
31. Mehrpouya, M.; Edelijn, T.; Ibrahim, M.; Mohebsahedin, A.; Gisario, A.; Barletta, M. Functional behavior and energy absorption characteristics of additively manufactured smart sandwich structures. *Adv. Eng. Mater.* **2022**, 2200677. [[CrossRef](#)]
32. Bellini, A.; Güçeri, S. Mechanical characterization of parts fabricated using fused deposition modeling. *Rapid. Prototyp. J.* **2003**, *9*, 252–264. [[CrossRef](#)]
33. Ahn, S.H.; Montero, M.; Odell, D.; Roundy, S.; Wright, P.K. Anisotropic material properties of fused deposition modeling abs. *Rapid. Prototyp. J.* **2002**, *8*, 248–257. [[CrossRef](#)]
34. Akhoundi, B.; Behraves, A.H. Effect of filling pattern on the tensile and flexural mechanical properties of fdm 3d printed products. *Exp. Mech.* **2019**, *59*, 883–897. [[CrossRef](#)]
35. Phadke, M.S. *Quality Engineering Using Robust Design*; Prentice Hall PTR: Englewood Cliffs, NJ, USA, 1995.
36. Roy, R.K. *A Primer on the Taguchi Method*; Society of Manufacturing Engineers: Southfield, MI, USA, 2010.
37. Ouballouch, A.; Lasri, L.; Ouahmane, I.; Sallaou, M.; Ettaqi, S. Optimization of pla parts manufactured by the fused deposition modeling technology. In Proceedings of 2018 IEEE International Conference on Technology Management, Operations and Decisions (ICTMOD), Marrakech, Morocco, 21–23 November 2018; pp. 288–292. [[CrossRef](#)]
38. Rajpurohit, S.R.; Dave, H.K. Analysis of tensile strength of a fused filament fabricated pla part using an open-source 3d printer. *Int. J. Adv. Manuf. Tech.* **2019**, *101*, 1525–1536. [[CrossRef](#)]